Available online at www.sciencedirect.com
ScienceDirect
Journal of Photochemistry and Photobiology A: Chemistry 190 (2007) 41–44
Journal of Photochemistry and Photobiology A:Chemistry
www.elsevier.com/locate/jphotochem

Reverse saturable absorption dynamics in indocyanine green

L. De Boni, D.C.J. Rezende, C.R. Mendonça*

Instituto de Física de São Carlos, Universidade de São Paulo, Caixa Postal 369,
13560-970 São Carlos, SP, Brazil

Received 5 October 2006; received in revised form 9 March 2007; accepted 11 March 2007
Available online 14 March 2007

Abstract

In this work, we studied the nonlinear absorption dynamics of indocyanine green (ICG) in dimethyl sulfoxide (DMSO) at 532 nm. Single pulse and pulse train Z-scan techniques were used to obtain singlet and triplet states dynamics, which were analyzed with a three- and five-energy level diagram, respectively. The excited singlet state absorption cross-section was determined to be 75 times higher than the ground state one, giving rise to reverse saturated absorption. Reverse saturated absorption also occurs from the triplet state, after its population through an intersystem crossing process, whose characteristic time is 4 ns. The triplet state absorption cross-section determined is 31 times higher than the ground state one. The high excited singlet and triplet states absorption cross-sections of ICG indicates its use in application requiring reverse saturated absorption, such as sensitizer for photodynamic therapy and optical limiting.

Keywords: Optical limiting; Photo-sensitizer; Pulse train Z-scan technique; Nonlinear optics

1. Introduction

Organic materials exhibit several interesting linear and nonlinear optical properties, which can be further modified or optimized through changes in their molecular structures. For example, some organic compounds possessing reverse saturated absorption (RSA) have been studied for applications in optical limiting [1–4] and optical switches [5]. The RSA process occurs when the absorption cross-section of the excited state is higher than that of the ground state. For macrocyclic compounds, such as porphyrins and phthalocyanines, after the molecule excitation to a singlet state, a conversion to a triplet state takes place, contributing additively to the RSA process.

The organic dye ICG has many applications. It can be applied in optical limiting devices [3] due to its efficient RSA. Indocyanine green can also be used as laser dye [6] and as saturable absorber [7]. In medicine, ICG has been used for diagnosis [8] and photodynamic therapy (PDT) of cancer [9,10]. The PDT mechanism involves the interaction of triplet state molecules with triplet oxygen, resulting in singlet oxygen, an active agent that destroys tumor cells. In this way, sensitizers with high rates of conversion to the triplet state are required. Fundamental studies on absorption and emission spectroscopy of ICG have already been reported [11]. The dependence of $S_1 \rightarrow S_0$ transition lifetime (τ_{10}), intersystem crossing time and quantum yield of triplet formation of ICG in different solvents were investigated [12,13]. These results showed that the conversion efficiency to the triplet state is diminished by increasing the solvent polarity. The same behavior was observed for the τ_{10}. For instance, in DMSO (an apolar solvent), τ_{10} time is 30-fold greater than that observed in polar solvents.

To further understand the excited states features (singlet and triplet absorption cross-sections and intersystem crossing time), the present work investigates ICG solution in DMSO. To perform this study, we employed the single pulse [14] and pulse train Z-scan (PTZ-scan) [15] techniques, both at 532 nm. Using the single pulse Z-scan and a theoretical analysis employing a three-energy level diagram, we determined the excited singlet absorption cross-section. On the other hand, with the PTZ-scan technique and a five-energy level diagram, we obtained the intersystem crossing time [16,17] and the triplet absorption cross-section. This methodology, which employs two distinct pulse configurations, diminished the number of fitting parameters and improves its accuracy.

---

* Corresponding author. Tel.: +55 16 3373 8085; fax: +55 16 3373 8085.
E-mail address: crmendon@if.sc.usp.br (C.R. Mendonça).

1010-6030/$ – see front matter © 2007 Elsevier B.V. All rights reserved.
doi:10.1016/j.jphotochem.2007.03.010

2. Experiments

In order to measure the nonlinear properties of ICG, we prepared DMSO solution in a concentration of 1.2×10^{17} molecules/cm^3. The UV–vis absorption spectrum was obtained with a Cary-17A spectrometer at room temperature, with a concentration six times smaller than that used in the nonlinear optical measurements. The linear and nonlinear measurements were carried out in a quartz cuvette with 2 mm of optical path.

Two configuration of the Z-scan technique were employed to investigate the optical nonlinearities. The first one was the traditional single pulse Z-scan technique [14], that basically consists in translating the sample through the focal plane of a Gaussian beam, while changes in intensity are monitored in the far-field. The second configuration used was the PTZ-scan (Z-scan with pulse train) technique [15], which is able to verify nonlinear dynamics in the nanosecond time scale. The experimental apparatus of this method is similar to the traditional one. In this case, however, while the sample is moved along the focal plane, the pulse train of a Q-switched/mode-locked laser is acquired. The amplitudes of each individual pulse in the train are normalized to the ones obtained when the sample is far from the focus. In both the configurations, the sample excitation was performed at 532 nm, the second harmonic of a Nd:YAG Q-switched and mode-locked laser. For the PTZ-scan method a pulse train with about 20 pulses, each one with ∼100 ps, separated by 13 ns was employed. For single pulse Z-scan, a Pockels cell between two crossed polarizes was used to extract one pulse from the pulse train. Single pulse and pulse train measurements were made with the laser operating at a 10 Hz repetition rate to eliminate accumulative thermal effects.

3. Results and discussion

Fig. 1 shows the molecular structure (inset) and the linear absorption spectra of ICG diluted in DMSO. It has a strong band around 800 nm, related to the $\pi \rightarrow \pi^*$ transition. At 532 nm, wavelength employed in the nonlinear optical measurements, only a small absorption was observed.

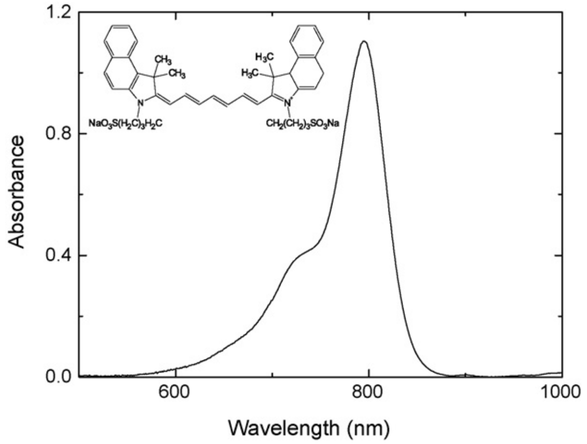

Fig. 1. Absorption spectrum of indocyanine green in DMSO for a concentration of 2×10^{16} molecules/cm^3. The inset shows the molecular structure of ICG.

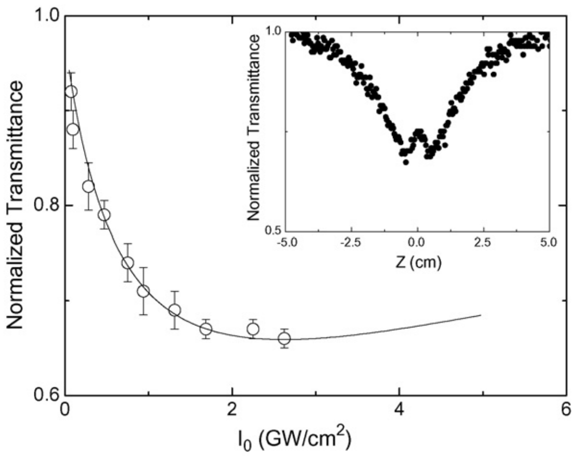

Fig. 2. Normalized transmittance as a function of pulse irradiance for ICG in DMSO. The solid line represents the fitting obtained with three-energy level diagram. The inset shows an open aperture Z-scan signature.

Fig. 2 shows the decrease of the normalized transmittance (NT) as a function of pulse irradiance, characterizing a RSA process. Each point in Fig. 2 corresponds to the minimum value extracted from single pulse open-aperture Z-scan measurements, illustrated in the inset of Fig. 2. The Z-scan curve was measured with a pulse irradiance of 3.4 GW/cm^2.

We also observed a saturation of the NT due to the accumulation of molecules in the first singlet excited state (S_1) and to the depleting of the ground state (S_0). As seen in Fig. 2, the saturation for ICG in DMSO occurs at ∼2 GW/cm^2, a relatively low intensity for this type of nonlinear process. This low saturation intensity for ICG is related to its $S_1 \rightarrow S_0$ transition lifetime ($\tau_{10} \sim 700$ ps) [12], which allows a considerable accumulation of ICG molecules in the singlet excited state (S_1). With more molecules in the first excited state, more transitions occur to the second excited state (S_2), that presents an absorption cross-section approximately null. This process can be visualized by the increase in the NT curve fitting that occurs after about 3 GW/cm^2 in Fig. 2. Furthermore, this effect can also be noticed through the Z-scan signature (inset of Fig. 2), where an increase in the NT at the focal position was observed.

In order to fit the experimental data obtained with the single pulse Z-scan technique (Fig. 2), the three-energy level diagram showed in Fig. 3(i), representing only the singlet states (S) of the molecule was employed. As the band gap of ICG is around 1.5 eV, the internal conversion process must be taken in account [18] into the rate equations to describe the population dynamics and obtaining the spectroscopic parameters. The triplet states

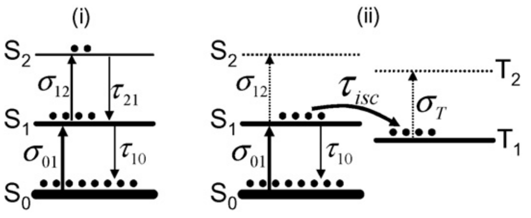

Fig. 3. Three- (i) and five- (ii) energy level diagram used to model the single pulse and pulse train Z-scan results.

were neglected, because the duration of each single pulse is shorter than the intersystem crossing time. In this case, only the singlet states contribute to the nonlinear absorption process. The transition lifetime (τ_{10}) can be described by $1/\tau_{10} = 1/\tau_r + 1/\tau_{ic}$, where $\tau_r \approx 5.5$ ns [12] and $\tau_{ic} \approx 840$ ps (calculated from data at Ref. [12]) are singlet radiative lifetime and internal conversion time, respectively.

We also assumed that the lifetime of the second excited singlet state, τ_{21}, is in the order of a few femtoseconds; therefore, the population of this state is small at low irradiances. Hence, to describe the fraction of molecules in each state, we used the rate equation, given by:

$$\frac{dn_0}{dt} = -w_{01}n_0 + \frac{n_1}{\tau_{10}} \quad (1)$$

$$\frac{dn_1}{dt} = +w_{01}n_0 - w_{12}n_1 - \frac{n_1}{\tau_{10}} + \frac{n_2}{\tau_{21}} \quad (2)$$

$$\frac{dn_2}{dt} = +w_{12}n_1 - \frac{n_2}{\tau_{21}} \quad (3)$$

where n_i are the population fractions of the singlet states (S_i) with $n_0 + n_1 + n_2 = 1$. The $w_{01} = \sigma_{01}I(t)/h\nu$ and $w_{12} = \sigma_{12}I(t)/h\nu$ are the one-photon transition rates, with σ_{01} and σ_{12} being the ground and first state absorption cross-sections at 532 nm, respectively. The set of differential equations are numerically solved using a Gaussian temporal profile for the laser pulse. The time dependence of absorption coefficient during the excitation is given by:

$$\alpha(t) = N\{n_0(t)\sigma_{01} + n_1(t)\sigma_{12}\} \quad (4)$$

where N is the concentration. The transmittance can be calculated by integrating the Beer's law, $dI/dz = -\alpha(t)I(t)$, over the sample thickness and the full pulse width (over t from $-\infty$ to $+\infty$), once in our Z-scan experiments the detection system measures the pulse fluence. This result is then normalized to the linearly transmitted energy, $\varepsilon = \varepsilon_0 \exp\{-\alpha_{01}L\}$, and used to fit the data in Fig. 2 (solid line). The absorption coefficient, α_{01}, is obtained from the linear absorption spectrum and it is directly connected with the ground state absorption cross-section by $\sigma_{01} = \alpha_{01}N$. In this way, the only adjustable parameter in this fitting procedure is σ_{12}. The value determined from the fitting was $\sigma_{12} = (12 \pm 1) \times 10^{-17}\,\text{cm}^2$, which is 75 times higher than the ground state cross-section ($\sigma_{01} = 0.16 \times 10^{-17}\,\text{cm}^2$).

In Fig. 4, we display the accumulative nonlinearity for ICG obtained with PTZ-scan. As seen, the NT decreases with the pulse number up to about 10, after which a small increase can be observed. This behavior could be understood by using a five-energy level diagram (Jablonsky diagram), shown in Fig. 3(ii). When excited by a pulse of the train to the level S_1, the molecule can undergo an intersystem crossing to the triplet state T_1, return to the ground state S_0 or be promoted to a second excited state S_2. With the arrival of the next pulse of the envelope, accumulative contributions to the optical nonlinearity due to population built up at the long-lived (∼μs) T_1 state start to appear. The molecules in this state can be promoted to a second triplet state, T_2, resulting in a change in the molecule absorption. Given the low irradiance of each individual pulse of the train and short lifetime of the levels S_2 and T_2, their population can be neglected. Considering this model, the fraction of molecules in each state is given by:

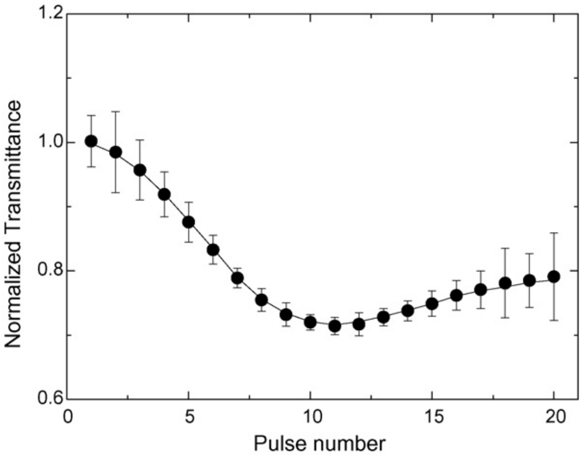

Fig. 4. Normalized transmittance along the Q-switch envelope for DMSO, obtained with an intensity of $I = 0.63\,\text{GW/cm}^2$. The solid line represents the theoretical curve obtained with parameters given in the text, using the five-energy level diagram.

$$\frac{dn_0}{dt} = -w_{01}n_0 + \frac{n_1}{\tau_{10}} \quad (5)$$

$$\frac{dn_1}{dt} = w_{01}n_0 - \frac{n_1}{\tau_f} \quad (6)$$

$$\frac{dn_{T_1}}{dt} = \frac{n_1}{\tau_{isc}} \quad (7)$$

where n_{T_1} is the population fraction of the first triplet state, with $n_0 + n_1 + n_{T_1} = 1$ (normalization condition). The $S_1 \to S_0$ transition lifetime τ_{10} is given by $1/\tau_{10} = 1/\tau_f - 1/\tau_{isc}$, where τ_f and τ_{isc} are the fluorescence lifetime and the intersystem crossing time, respectively [12]. This set of equations was numerically solved, using the temporal intensity pattern of the Q-switched/mode-locked pulsed train, in order to determine the population of molecules in each state. The time evolution of the absorption can be calculated using:

$$\alpha(t) = N\{n_0(t)\sigma_{01} + n_1(t)\sigma_{12} + n_{T_1}(t)\sigma_T\} \quad (8)$$

where σ_T is the triplet state transition absorption cross-section. Following the same procedure previously described, using the Beer's law, we are able to determine the sample transmittance evolution. With this method the only adjustable parameters are σ_T and σ_{isc}, once σ_{01} and σ_{12} are already known (single pulse analysis). The solid line in Fig. 4 represents the best fittings obtained.

The intersystem crossing time obtained through the fitting was $\tau_{isc} \approx 4 \pm 1$ ns, which is in good agreement with the one reported in Ref. [12]. The quantum yield of triplet formation, ϕ_T, was calculated using $\phi_T = \tau_f/\tau_{isc}$ [16,17] and the previous value for τ_{isc}, providing $\phi_T \approx 15\%$. The absorption cross-section of the triplet state found through the fitting was $\sigma_T = (5 \pm 1) \times 10^{-17}\,\text{cm}^2$. This value is 31 ($\sigma_{01} = 0.16 \times 10^{-17}\,\text{cm}^2$) times higher than the ground state cross-section. We observed that

Table 1
Cross-section values ($\times 10^{-17}$ cm^2) for ground (σ_{01}), excited state (σ_{12}) and excited triplet (σ_T) states at 532 nm

σ_{01}	σ_{12}	σ_T	τ_f	ϕ_{fl}	ϕ_T	ϕ_{ic}	k_{isc}	k_r	k_{ic}
0.16	12 ± 1	5 ± 0.5	580 ± 40	0.106	0.15 ± 0.04	0.74 ± 0.05	2.5 ± 0.6	1.82 ± 0.07	11 ± 1

S_1 state lifetime (τ_f) (ps) [12], fluorescence (ϕ_f) [12], triplet (ϕ_T) and internal conversion (ϕ_{ic}) quantum yields and rate constants ($\times 10^8$ s^{-1}) of intersystem crossing (k_{isc}), radiative (k_r) [12] and internal conversion (k_{ic}) of ICG/DMSO solution.

σ_{12} is higher than σ_T for ICG ($\sigma_{12}/\sigma_T \sim 2.4$), indicating that the excited singlet state gives a higher contribution to the RSA process for ICG. In Table 1 are shown the spectroscopic parameters obtained by fitting single and pulse train Z-scan data. This table also shows ICG spectroscopic parameters from literature.

Attempts were also made to study the nonlinear absorption process of ICG dissolved in water. However, we observed changes in the linear absorption spectrum over time, indicating that ICG in aqueous solution is unstable due to its degradation and aggregation [19,20], which hinders the use of our Z-scan method which takes a few hours.

In summary, we observed a RSA behavior at 532 nm for ICG in DMSO solution. For single pulse experiments, we determined that the excited singlet state cross-sections was 75 times higher than those of the ground state. However, when pulse trains were employed, triplet population was identified, with an intersystem crossing time in the nanosecond time scale. In this case, the triplet absorption cross-sections found was 31 times higher than the ground state ones. These results indicate ICG as an interesting candidate for applications requiring RSA.

Acknowledgements

Financial support from FAPESP (Fundação de Amparo à Pesquisa do estado de São Paulo) and CNPQ (Conselho Nacional de Desenvolvimento Científico e Tecnológico) are gratefully acknowledged.

References

[1] M. Calvete, G.Y. Yang, M. Hanack, Synth. Met. 141 (2004) 231.
[2] J.W. Perry, Nonlinear Optics of Organics Molecules and Polymers, CRC Press, New York, 1997.
[3] S.M. O'Flaherty, S.V. Hold, M.J. Cook, T. Torres, Y. Chen, M. Hanack, W.J. Blau, Adv. Mater. 15 (2003) 19.
[4] D.S. Correa, L. De Boni, D.S. dos Santos, N.M.B. Neto, O.N. Oliveira, L. Misoguti, S.C. Zilio, C.R. Mendonca, Appl. Phys. B Lasers Opt. 74 (2002) 559.
[5] M.O. Liu, C.H. Tai, A.T. Hu, T.H. Wei, J. Organomet. Chem. 689 (2004) 2138.
[6] B.M. Pierce, R.R. Birge, IEEE J. Quantum Electron. 18 (1982) 1164.
[7] S. Oda, Y. Segawa, N. Kodama, P.H. Kim, S. Namba, Jpn. J. Appl. Phys. 2 28 (1989) L1977.
[8] I.J. Fox, E.H. Wood, Mayo Clin. Proc. 35 (1960) 732.
[9] W. Baumler, C. Abels, S. Karrer, T. Weiss, H. Messmann, M. Landthaler, R.M. Szeimies, Br. J. Cancer 80 (1999) 360.
[10] S. Fickweiler, R.M. Szeimies, W. Baumler, P. Steinbach, S. Karrer, A.E. Goetz, C. Abels, F. Hofstadter, M. Landthaler, J. Photochem. Photobiol. B-Biol. 38 (1997) 178.
[11] R. Philip, A. Penzkofer, W. Baumler, R.M. Szeimies, C. Abels, J. Photochem. Photobiol. A-Chem. 96 (1996) 137.
[12] S. Reindl, A. Penzkofer, S.H. Gong, M. Landthaler, R.M. Szeimies, C. Abels, W. Baumler, J. Photochem. Photobiol. A-Chem. 105 (1997) 65.
[13] H. Gratz, A. Penzkofer, C. Abels, R.M. Szeimies, M. Landthaler, W. Baumler, J. Photochem. Photobiol. A-Chem. 128 (1999) 101.
[14] M. Sheik-Bahae, A.A. Said, T.H. Wei, D.J. Hagan, E.W. Van Stryland, IEEE J. Quantum Electron. 26 (1990) 760.
[15] L. Misoguti, C.R. Mendonça, S.C. Zilio, Appl. Phys. Lett. 74 (1999) 1531.
[16] P.J. Goncalves, L. De Boni, N.M.B. Neto, J.J. Rodrigues, S.C. Zilio, I.E. Borissevitch, Chem. Phys. Lett. 407 (2005) 236.
[17] P.J. Gonçalves, L.P.F. Aggarwal, C.A. Marquezin, A.S. Ito, L.D. Boni, N.M.B. Neto, J.J.R. Jr, S.C. Zílio, I.E. Borissevitch, J. Photochem. Photobiol. A-Chem. 181 (2006) 137.
[18] N.J. Turro, Modern Molecular Photochemistry, Benjamin/Cummings Pub. Co., Menlo Park, California, 1978.
[19] F.J. Green, The Sigma–Aldrich Handbook of Stains, Dyes, and Indicators, Aldrich Chemical Co., Milwaukee, Wisconsin, 1990.
[20] M. Mauerer, A. Penzkofer, J. Zweck, J. Photochem. Photobiol. B-Biol. 47 (1998) 68.